JOURNAL OF RESEARCH of the National Bureau of Standards — C. Engineering and Instrumentation
Vol. 71C, No. 2, April–June 1967

The Sensitivity of the Dicke Radiometer*

David F. Wait**

Institute for Basic Standards, National Bureau of Standards, Boulder, Colo. 80302

(January 25, 1967)

The literature is reviewed concerning the sensitivity of the Dicke radiometer, excluding gain fluctuations. Discrepancies are pointed out and a new derivation of sensitivity using a Fourier transform method is used to resolve these discrepancies and to extend the results to radiometers with lossy switches.

Experimentally it is shown that radiometers using a half-wave square-law, linear-law, intermediate-law, or envelope detectors all have a sensitivity equal to the theoretical full-wave square-law detector (within the ±20 percent uncertainty of the experiment).

Key Words: Dicke, microwave, radiometer, sensitivity, switching.

1. Introduction

At the National Bureau of Standards a switching radiometer is used to compare microwave noise sources with a standard hot load [1],[1] and a sum-and-difference-correlation radiometer is being developed to compare microwave cryogenic noise sources which uses a switching radiometer as a component [2].

Although there is extensive literature discussing the Dicke radiometer, existing publications are difficult to use. This is partly due to a series of errors and corrections and partly due to divergent assumptions, notation, and forms. The literature as a whole has unresolved differences between various statements of the sensitivity for the Dicke radiometer.

The purpose of this paper is to review the literature (sec. 2), derive the sensitivity of the Dicke radiometer in a form which includes switch noise (sec. 3), and to compare the derived sensitivity with experiment (sec. 4). The sensitivity is rederived, rather than making a further correction, for two reasons. First, a statement of sensitivity is needed in a form general enough to include the prior literature. This facilitates identifying discrepancies. Second, a basically different derivation helps to avoid prior errors and to increase confidence where agreements are obtained.

2. Review of the Literature

To facilitate comparison between the various authors in the literature, a brief discussion of a model switching radiometer is presented. The literature is compared in terms of this model. The symbols of this paper may be converted to the notation of the other authors by means of appendix A. Also contained in appendix A are equivalent statements of predetector bandwidth B, and postdetector integration constant τ.

*Sponsored by Advanced Research Projects Agency, Project DEFENDER; ARPA Order No. 515.
**Microwave Circuit Standards, National Bureau of Standards Laboratories, Boulder, Colo. 80302.
[1] Figures in brackets indicate the literature references at the end of this paper.

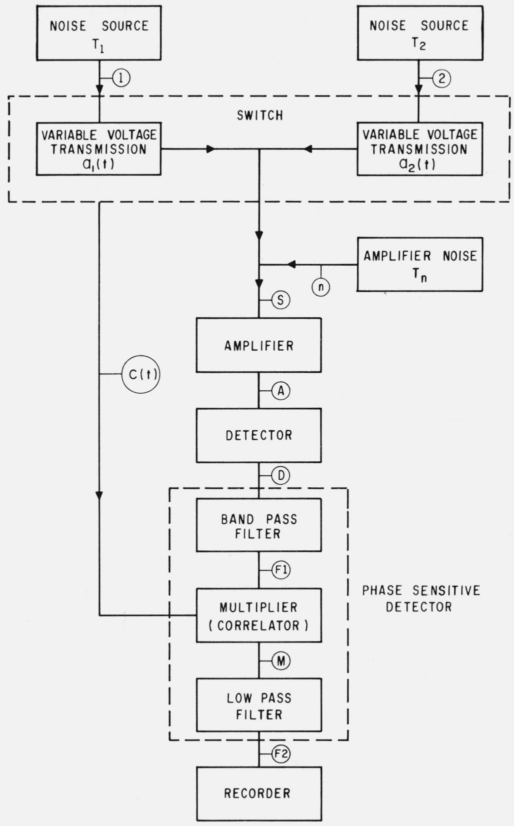

FIGURE 1. *Dicke radiometer.*

2.1. Basic Switching Radiometer

The basic switching radiometer is shown in figure 1. Essentially the power from a noise source at the effective temperature T_1 is compared with a noise source at effective temperature T_2. It is usually advantageous to operate the radiometer with a known and variable T_2 which is made equal to T_1. The comparison of T_1 to T_2 is effected by switching the input of a receiver from T_1 to T_2 and examining the output of the receiver for a signal correlated with the switching frequency. Uncorrelated terms (for example, the internal noise of the receiver) do not contribute to the dc output of the correlator.

The noise voltage $y_1(t)$ from the noise source at temperature T_1 is connected to the receiver through a variable coupler of voltage transmission coefficient $a_1(t)$. Similarly $y_2(t)$ from noise source T_2 is fed through a variable coupler with voltage transmission coefficient $a_2(t)$. The internal noise of the amplifier referred to the input of the amplifier has effective temperature T_n. The signal $y_s(t)$, the input to an ideal noiseless amplifier, is

$$y_s(t)=a_1(t)y_1(t)+a_2(t)y_2(t)+y_n(t), \tag{1}$$

where $y_n(t)$ is the voltage needed to represent the amplifier noise. Ideally the transmission coefficients $a_1(t)$ and $a_2(t)$ vary from zero to one periodically with period ν_0^{-1}. Typically $a_1(t)$ and $a_2(t)$ are 180° out of phase. The transmission coefficient $a_1(t)$ is referred to as the *voltage modulation.* The power transmission coefficient $p(t)\equiv a^2(t)$ is referred to as the *power modulation.* From the modulation $a_1(t)$ is generated a periodic reference signal $c(t)$ which then goes to the multiplier. The reference signal $c(t)$ is referred to as the *correlation* and usually is sinusoidal or square wave.

2.2. General Comments

Eleven papers (as noted in table 1) are here reviewed which contain statements concerning the sensitivity of a Dicke radiometer. There is an underlying agreement among eight of these and the remaining three retain many of the essential features. In order to recognize this agreement, various definitions must be related (see appendix A) and account taken of the modulation and correlation assumed.

There is an important difference among the various agreeing papers. The nature of this difference is essential to the general understanding of the literature, so it will be discussed before commenting on individual papers.

The radiometer described by Dicke [3] modulates the noise source by means of a variable attenuator which has nearly the same temperature as the noise source of interest. The papers of Goldstein [4, 5], Strom [6, 7], Strum [8], Knight [9], and Johnson [10], collectively referred to as GSSKJ, calculate the sensitivity of a somewhat different radiometer. The GSSKJ version of the Dicke radiometer modulates the noise source of interest by an ideal noiseless device, which could be a variable attenuator at the absolute zero of temperature. This corresponds to $T_2 \equiv 0$ °K in the model introduced in section 2.1. The Dicke radiometer was originally a null device but this concept was extended by Goldstein to include an off-null operation. This introduces many practical differences. For example, a radiometer operated off-null is not immune from receiver gain instabilities. The radiometer described by GSSKJ is a special case of the papers of Kelly, Lyons and Root [11, 12], Colvin [13], and Tiuri [14] collectively referred to as KLRCT. However, GSSKJ and KLRCT differ in detail. For example, GSSKJ's results indicate somewhat greater fluctuations in the radiometer output due to the input noise source (T_1) than the corresponding KLRCT results.

The origin of the discrepancy lies in the different technique of obtaining the output of the square law detector relative to the input. GSSKJ use an autocorrelation method and handle the resulting squared terms by means of a theorem usually attributed to Rice [15]. Rice's theorem for square law devices is rigorous for stationary Gaussian processes. KLRCT essentially apply Rice's theorem directly, neglecting the usually small nonstationary aspect of the signal at the detector input. The errors introduced by this simplifying assumption go to zero as the noise sources being compared approach the same temperature ($T_1 = T_2$), and the receiver is switched between the two sources in such a way that the power to the receiver is constant throughout the switching cycle.

The calculations in this paper are as precise as the GSSKJ calculations. Thus detailed agreement with KLRCT is expected only when $T_1 = T_2$.

In the last column of table 1, which appears later in this paper, prior calculations of the radiometer sensitivity are indicated by modulation and correlation type. Those calculations which differ with this paper are marked with an asterisk. Although Goldstein [4, 5], Strum [8], and Knight [9] are marked with an asterisk, they are considered to be in the group of eight having underlying agreement. More will be said of this in the detailed comments which follow.

2.3. Specific Comments

In 1946, Dicke [3] suggested modulating a noise signal under study as a means of distinguishing the signal of interest from the noise originating in the amplifying system and also to reduce the fluctuations in the radiometer output due to receiver gain instabilities. He derived the sensitivity of a radiometer using a statistical approach for square-wave modulation and sinusoidal correlation. In the analysis Dicke assumed that the detector was square-law, then he generalized to the linear detector. Selove [16] corrects an error in the generalization to the linear detector and Strom [6, pp 37 and 68] challenges an overall factor. For a square-wave modulation and sinusoidal correlation, Dicke obtained a sensitivity which is a factor of 2 greater than the result to be obtained in this paper and thus comparable with the accepted sensitivity of an ideal (no gain fluctuations) total power radiometer [11, 12, 13, or 14]. Because the switching radiometer cannot have comparable sensitivity, Dicke's result must be in error.

In 1955, Goldstein [4] analyzed the switching radiometer using sinusoidal-voltage modulation (or switching), sinusoidal correlation and square-law detection making use of the autocorrelation function and assuming the noise signal had a Gaussian distribution. However, as noted above, he assumed a noiseless modulator which corresponds to assuming $T_2 \equiv 0$ °K. Goldstein's result as corrected by himself [5] and Johnson [10] agrees with a special case of the analysis to be presented.

Also in 1955 Bunkin and Karlov [17] analyzed the switching radiometer using the autocorrelation method. Their analysis assumes a Gaussian noise distribution, square-wave modulation and sinusoidal correlation. In addition, the effects of amplifier gain fluctuations are considered. This paper depends to some extent on other papers in the Russian literature which are not readily available. It was not established for certain if the paper agrees in all details, but no obvious discrepancies occur.

Strom [6, 7] shows that the sensitivity of the switching radiometer is unaltered if a biased diode is used as the detector instead of a square-law detector. He obtains a sensitivity that is less by a factor $\sqrt{2}$ than the expected value because the out-of-phase rejection of noise by the correlator was not taken into account.

Strum [8] discusses the effect of fluctuations in various components of a radiometer system and discusses various types of linear detectors. He comments on the use of an IF amplifier in an analysis. Strum defines a generalized bandwidth which reduces to the usual one for rectangular bandpass but is not equivalent in general to that used by Dicke; Kelly, Lyons, and Root; Ward and Richardson; Tiuri; and in this paper.

Kelly, Lyons, and Root [11, 12] analyzed a general comparison radiometer (T_1 and T_2 arbitrary) for arbitrary modulation and correlation. They treated gain fluctuations and optimized the modulation wave form depending on the rms amplitude of the gain fluctuations. They also presented a proof that a square-law detector is superior to any other detector law for Gaussian noise (ignoring gain fluctuation of the amplifier). Except for the differences off-null already noted, there is no disagreement with this paper.

Colvin [13] discusses the switching radiometer under rather general conditions as part of an extensive survey of various radiometers. Again, except for the off-null differences discussed, there is no disagreement with this paper.

Knight [9] considers a radiometer with asymmetrical rectangular modulation and correlation. The calculation is of the Goldstein type. In his paper, eqs (3) and (4) lack the factor 2π on the right-hand side which occurred in his prior equations. Knight's corrected equations are a special case of the analysis to be presented. However, his extension to the balanced radiometer operation did not take into account the fluctuation of the output due to the noise sources.

Ward and Richardson [18] consider a power sinusoidal modulated radiometer with IF amplifiers of different image and signal responses. The sensitivity obtained is that expected for a total power radiometer, and for the same reason as noted for Dicke's paper, this must be in error.

Johnson [10] corrected Goldstein's results and extended the calculation to include various combinations of sinusoidal and square-wave modulations and correlations. However, in Johnson's extension to square-wave modulation his (1/4) $\sigma_s^2\sigma_n^2$ term should be replaced by $\sigma_s^2\sigma_n^2$.[2]

Tiuri [14] states the radiometer sensitivity for several modulations and correlations. The results are the expected ones within the approximations already discussed.

3. Analysis

The sensitivity of the switching radiometer depicted in figure 1 is determined by calculating the ratio of the dc output of the radiometer $\overline{y_{F2}}$ and the rms fluctuations at the output, σ_{F2}. The time dependent noise voltages will be denoted by $y(t)$ with a subscript denoting the point in the circuit shown in the circles in figure 1. An IF amplifier is not used in figure 1 but is treated in appendix C.

[2] This has been acknowledged by Johnson in a private communication.

3.1. The Fourier Transform

The Fourier transform preserves required phase information. Because the transform of a random function does not converge, all the noise voltages $y(t)$ are defined to be zero except for $-T/2 < t < T/2$. The truncated function of $y(t)$ has identical properties with $y(t)$ in the limit $T \to \infty$. Thus by $y(t)$ it will be understood the truncated function of $y(t)$. The Fourier transform of $y(t)$ is denoted $Y(\nu)$, again with a subscript to denote point in the circuit.

The following form is used for the Fourier transform pair:

$$Y(\nu) = \int_{-\infty}^{\infty} e^{-j2\pi\nu t} y(t)\, dt, \tag{2}$$

$$y(t) = \int_{-\infty}^{\infty} e^{j2\pi\nu t} Y(\nu)\, d\nu. \tag{3}$$

The Fourier transform or inverse transform of a product (in either t or ν space) is the convolution of the transforms of the two factors (convolution theorem). With the choice in (2) and (3), the convolutions (denoted by ★) are defined by

$$y_x(t) \bigstar y_z(t) \equiv \int_{-\infty}^{\infty} y_x(t-t') y_z(t')\, dt', \tag{4}$$

and

$$Y_x(\nu) \bigstar Y_z(\nu) \equiv \int_{-\infty}^{\infty} Y_x(\nu-\nu') Y_z(\nu')\, d\nu'. \tag{5}$$

3.2. The Power Spectral Density and the Wiener-Khintchine Theorem

The power spectral density $W(\nu)$ is related to the Fourier transform of $y(t)$ in the following manner [19],

$$W(\nu) = \operatorname*{Lim}_{T\to\infty} \frac{Y(\nu) Y^*(\nu)}{T}, \tag{6}$$

where the asterisk denotes the complex conjugate. It can be shown that $W(\nu)d\nu$ is the power dissipated in a 2-Ω resistor due to the spectral components between ν and $\nu + d\nu$ in the voltage $y(t)$.

The Wiener-Khintchine Theorem is stated [20]

$$W(\nu) = \int_{-\infty}^{\infty} R(t) e^{-j2\pi\nu t}\, dt, \tag{7}$$

so that

$$R(t) = \int_{-\infty}^{\infty} W(\nu) e^{j2\pi\nu t}\, d\nu, \tag{8}$$

where $R(t)$ is the autocorrelation function defined by

$$R(t) \equiv \operatorname*{Lim}_{T\to\infty} \frac{1}{T} \int_{-T/2}^{T/2} y(t') y(t'+t)\, dt'. \tag{9}$$

Using (8) and (9) for $t=0$,

$$\overline{y^2(t)} = \int_{-\infty}^{\infty} W(\nu)\, d\nu, \tag{10}$$

where the bar indicates the time average in the interval $-T/2$ to $+T/2$.

The analysis is ultimately stated in terms of measurable properties of the input noise signals [21, 22]:

$$W_1(\nu)=\frac{1}{2}\,kT_1,$$

$$W_2(\nu)=\frac{1}{2}\,kT_2, \tag{11}$$

$$W_n(\nu)=\frac{1}{2}\,kT_n,$$

where $k=1.3805\times10^{-23}$ J °K^{-1} is the Boltzmann constant. The factor 1/2 in (11) occurs because the power spectral density is defined for both positive and negative frequencies.

3.3. The Switch

A model for the switch discussed in section 2.1 led to eq (1). For this analysis a more general $y_s(t)$ composed of an arbitrary number of periodically modulated noise signals will be used. The voltage modulation of the ith signal $[a_i(t)]$ is analyzed into its Fourier components:

$$a_i(t)=\sum_m A_{j,\,m}e^{jm2\pi\nu_0t}, \tag{12}$$

where m takes all integer values between $-\infty$ and $+\infty$. Similarly the correlation signal is decomposed:

$$c(t)=\sum_m C_m e^{jm2\pi\nu_0t}. \tag{13}$$

The following associated transmission coefficients are also required:

$$p_i(t)\equiv a_i^2(t), \tag{14}$$

$$q_i(t)\equiv p_i^2(t)=a_i^4(t), \tag{15}$$

$$u_{ij}(t)\equiv a_i(t)a_j(t), \tag{16}$$

$$v_{ij}(t)\equiv a_i^2(t)a_j^2(t), \tag{17}$$

which are decomposed into

$$p_i(t)=\sum_m P_{i,\,m}e^{jm2\pi\nu_0t}, \tag{18}$$

$$q_i(t)=\sum_m Q_{i,\,m}e^{jm2\pi\nu_0t}, \tag{19}$$

$$u_{ij}(t)=\sum_m U_{ij,\,m}e^{jm2\pi\nu_0t}, \tag{20}$$

and

$$v_{ij}(t)=\sum_m V_{ij,\,m}e^{jm2\pi\nu_0t}. \tag{21}$$

3.4. The $y(t)$, $Y(\nu)$, $W(\nu)$ Description

Each element of the radiometer depicted in figure 1 is described by the modification to $y(t)$ before and after the element. Thus,

$$y_S(t)=\sum_i a_i(t)y_i(t) \tag{22}$$

$$y_A(t)=h_A(t)\bigstar y_s(t), \tag{23}$$

$$y_D(t)=y_A^2(t), \tag{24}$$

$$y_{F1}(t)=h_{F1}(t)\bigstar y_D(t), \tag{25}$$

$$y_M(t)=c(t)y_{F1}(t), \tag{26}$$

$$y_{F2}(t)=h_{F2}(t)\bigstar y_M(t), \tag{27}$$

where $h_A(t)$, $h_{F1}(t)$, $h_{F2}(t)$ are the impulse response functions [20] of the amplifier, bandpass filter and low pass filter, respectively, and $c(t)$ is defined in (13).

Taking the Fourier transforms of (22) to (27) and using (12),

$$Y_S(\nu)=\sum_{i,\,m} A_{i,\,-m}Y_i(\nu+m\nu_0), \tag{28}$$

$$Y_A(\nu)=H_A(\nu)Y_S(\nu), \tag{29}$$

$$Y_D(\nu)=Y_A(\nu)\bigstar Y_A(\nu), \tag{30}$$

$$Y_{F1}(\nu)=H_{F1}(\nu)Y_D(\nu), \tag{31}$$

$$Y_M(\nu)=\sum_{m=-\infty}^{\infty} C_{-m}Y_{F1}(\nu+m\nu_0), \tag{32}$$

$$Y_{F2}(\nu)=H_{F2}(\nu)Y_M(\nu). \tag{33}$$

The Fourier transform of the impulse response function is known as the system function, or transfer function, denoted $H(\nu)$,

$$H(\nu)\equiv\int_{-\infty}^{\infty} e^{-j2\pi\nu t}h(t)dt, \tag{34}$$

and will be used to define the power response function $G(\nu)$,

$$G(\nu)\equiv H(\nu)H^*(\nu). \tag{35}$$

The power spectral density is obtained from (28) to (33) by means of (6) and (B–1) of appendix B. This results in

$$W_S(\nu)=\sum_{i,m} A_{i,-m}A^*_{i,-m}W_i(\nu+m\nu_0), \tag{36}$$

$$W_A(\nu)=G_A(\nu)W_S(\nu), \tag{37}$$

$$W_D(\nu)=\lim_{T\to\infty} T^{-1}Y_D(\nu)Y^*_D(\nu), \tag{38}$$

$$W_{F1}(\nu)=G_{F1}(\nu)W_D(\nu), \tag{39}$$

$$W_M(\nu)=\sum_{m=-\infty}^{\infty} C_{-m}C^*_{-m}W_{F1}(\nu+m\nu_0), \tag{40}$$

$$W_{F2}(\nu)=G_{F2}(\nu)W_M(\nu), \tag{41}$$

where $G_A(\nu)$ (see eq 35) is the power response of the amplifier, etc. The spectral density of $W_D(\nu)$ will not be deduced from $W_A(\nu)$ due to the complication arising from $W_A(\nu)$ being nonstationary.

3.5. Calculation of $\overline{y_{F2}}$

The calculation of $\overline{y_{F2}}$ (d-c output of the radiometer) is based on the following relationship (see appendix B):

$$\overline{y_{F2}}=\lim_{T\to\infty}\frac{Y_{F2}(0)}{T}. \tag{42}$$

Using (31) to (33),

$$Y_{F2}(0)=H_{F2}(0)\sum_{m=-\infty}^{\infty} C_{-m}H_{F1}(m\nu_0)Y_D(m\nu_0). \tag{43}$$

The task now is to obtain $Y_D(m\nu_0)$ in terms of the known power spectral densities of (11). The approach is to cast $Y_D(m\nu_0)$ in a form to utilize the relationship (see appendix B)

$$\lim_{T\to\infty}\frac{Y_{xx}(0)}{T}=K_x, \tag{44}$$

where

$$K_x\equiv\int_{-\infty}^{\infty} W_x(\nu)d\nu, \tag{45}$$

and $Y_{xx}(0)$ is the Fourier transform of $y_x^2(t)$ for $\nu=0$, where $y_x(t)$ is a noise function with zero mean.

If we assume a flat amplifier response so that $H_A(\nu+m\nu_0)\simeq H_A(\nu)$, then (29) may be written,

$$Y_A(\nu)\simeq\sum_{i,p} A_{i,-p}Y_{i\star A}(\nu+p\nu_0), \tag{46}$$

where $Y_{1\star A}(\nu)$ is the Fourier transform of $h_A(t)\bigstar y_1(t)$, etc. The approximation for the transfer function of the amplifier, $H_A(\nu)$ might seem unrealistic for large p, but generally $A_{i,p}$ decreases rapidly with increasing $|p|$.

Substituting (46) into (30) will give terms of the form

$$Y_x(\nu+p\nu_0)\bigstar Y_z(\nu+q\nu_0)=Y_{xz}(\nu+p\nu_0+q\nu_0), \tag{47}$$

where $Y_{xz}(\nu)$ is the Fourier transform of $y_x(t)y_z(t)$, x, z are any of the subscripts $1\bigstar A$, $2\bigstar A$ or $n\bigstar A$. Equation (47) is valid even when $x=z$. For a proof of (47) see appendix B.

We are now in a position to use (44) to facilitate the evaluation of (30). Because $Y_{xz}(\nu+p\nu_0+q\nu_0)$ gives no contribution except for $x=z$ and $\nu+p\nu_0+q\nu_0=0$ (see appendix B), then by retaining only nonzero terms and excluding $m=0$ (because $A_{i,\,0}=0$),

$$\lim_{T\to\infty}\frac{Y_D(m\nu_0)}{T}=\sum_{i,\,q}A_{i,\,q}A_{i,\,-q-m}K_{i\bigstar A}, \tag{48}$$

where from (6), (11), and (45), for $i=1$ or 2,

$$K_{i\bigstar A}=\frac{1}{2}kT_i\int_{-\infty}^{\infty}G_A(\nu)d\nu. \tag{49}$$

Thus, for the usual case that $C_0=0$, (42), (43), (48) and (49) combine to give,

$$\overline{y_{F2}}=\lambda B^{1/2}\left\{\sum_{i,\,m}C_mH_{F1}(m\nu_0)P_{i,\,-m}T_i\right\}, \tag{50}$$

where

$$\lambda=\frac{1}{2}\,kH_{F2}(0)\,[2G_A(0)\bigstar G_A(0)]^{1/2}, \tag{51}$$

and

$$B\equiv\frac{\left[\int_{-\infty}^{\infty}G_A(\nu)d\nu\right]^2}{2G_A(0)\bigstar G_A(0)}, \tag{52}$$

or using appendix A,

$$B=\frac{\int_{-\infty}^{\infty}G_A(\nu)\bigstar G_A(\nu)d\nu}{2G_A(0)\bigstar G_A(0)}, \tag{53}$$

and $P_{i,\,m}$ defined in (18) is introduced by means of (B–7) of appendix B. The term B is the convolution bandwidth of the amplifier. For a rectangular power response, B is the width of the nonzero response in hertz (cycles per second).

3.6. Calculation of σ_{F2}

The rms fluctuation (standard deviation) σ_{F2} is defined by

$$\sigma_{F2}^2=\overline{y_{F2}^2(t)}-\overline{y_{F2}(t)}^2.$$

The bar indicates the time average in the interval $-T/2$ to $T/2$. Using (10) this may be written,

$$\sigma_{F2}^2=\int_{-\infty}^{\infty}W_{F2}(\nu)d\nu-\overline{y_{F2}}^2.$$

If the δ-function term [23] from (38) is separated from $W_{F2}(\nu)$ of (41), denoted by a prime,

$$\sigma_{F2}^2 = \int_{-\infty}^{\infty} W'_{F2}(\nu)\, d\nu. \tag{54}$$

Combining (22), (23), and (24), and assuming the modulation frequency is small compared with the amplifier bandwidth so the modulation factor distortion is negligible, then

$$y_D(t) = \left[\sum_i a_i(t) y_{i\bigstar A}(t)\right]^2, \tag{55}$$

where

$$y_{i\bigstar A}(t) \equiv h_A(t) \bigstar y_i(t). \tag{56}$$

Expanding (55) and using (14) and (16),

$$y_D(t) = \sum_i p_i(t) y^2_{i\bigstar A}(t) + 2 \sum_{i<j} u_{ij}(t) y_{i\bigstar A}(t) y_{i\bigstar A}(t). \tag{57}$$

Taking the Fourier transform of (57), then using (6) and (B–2), to obtain the power spectral density,

$$W'_D(\nu) = \sum_{i,\,m} P_{i,\,-m} P^*_{i,\,-m} W'_{i\bigstar A,\,i\bigstar A}(\nu + m\nu_0) + 4 \sum_{i<j,\,m} U_{ij,\,-m} U^*_{ij,\,-m} W'_{i\bigstar A,\,j\bigstar A}(\nu + m\nu_0), \tag{58}$$

where $W_{i\bigstar A,\,j\bigstar A}(\nu)$ is the power spectral density of $y_{i\bigstar A}(t) y_{j\bigstar A}(t)$ and the primes indicate δ-function terms are omitted. It can be shown [15] that

$$W'_{i\bigstar A,\,i\bigstar A}(\nu) = 2[G_A(\nu) W_i(\nu)] \bigstar [G_A(\nu) W_i(\nu)], \tag{59}$$

where $G_A(\nu)$ is introduced in (37). Also for $i \neq j$,

$$W'_{i\bigstar A,\,j\bigstar A}(\nu) = [G_A(\nu) W_i(\nu)] \bigstar [G_A(\nu) W_j(\nu)]. \tag{60}$$

Using (59), (60), (10), (B–8), and (B–9) to simplify (58) and then using (39),

$$W'_{F1}(\nu) = \frac{1}{2} k^2 \left[\sum_i Q_{i,\,0} T_i^2 + 2 \sum_{i<j} V_{ij,\,0} T_i T_j\right] G_{F1}(\nu)[G_A(\nu) \bigstar G_A(\nu)], \tag{61}$$

where $Q_{i,\,0}$ and $V_{ij,\,0}$ are defined via (19) and (21).

For the computation of $W_{F2}(\nu)$ using (41), only $W_M(\nu)$ for $\nu \simeq 0$ will contribute because of the narrow low pass filter $F1$. Consequently in using (40) and (61), $G_{F1}(\nu \pm m\nu_0)[G_A(\nu \pm m\nu_0) \bigstar G_A(\nu \pm m\nu_0)]$ may be replaced by $G_{F1}(m\nu_0)[G_A(m\nu_0) \bigstar G_A(m\nu_0)]$ because the power transfer functions are even in ν. Furthermore, in the case where C_n decreases rapidly with increasing $|n|$, then to a good approximation $G_A(m\nu_0) \bigstar G_A(m\nu_0) \simeq G_A(0) \bigstar G(0)$. Therefore,

$$W'_{F2}(\nu) \simeq \frac{1}{2} \lambda^2 M^2 \left[\sum_i Q_{i,\,0} T_i^2 + 2 \sum_{i<j} V_{ij,\,0} T_i T_j\right] G_{F2}(\nu)/G_{F2}(0), \tag{62}$$

where λ is defined in (51) and

$$M \equiv \left[\sum_m C_{-m} C^*_{-m} G_{F1}(m\nu_0)\right]^{1/2}. \tag{63}$$

Thus using (54),

$$\sigma_{F2} \simeq \lambda M \tau^{-1/2} \left[\sum_i Q_{i,\,0} T_i^2 + 2 \sum_{i<j} V_{ij,\,0} T_i T_j \right]^{1/2} \tag{64}$$

where

$$\tau^{-1} \equiv \int_{-\infty}^{\infty} G_{F2}(\nu) d\nu / G_{F2}(0). \tag{65}$$

3.7. Sensitivity

A measure of a radiometer's sensitivity is $\sigma_{F2}^{-1}(d\overline{y_{F2}}/dT_1)$. It is customary to specify instead, the minimum resolvable change in T_1, denoted ΔT_{min}. Using the criterion that a change in $\overline{y_{F2}}$, denoted $\Delta\overline{y_{F2}}$ due to a change in T_1 is resolved when $\Delta\overline{y_{F2}} \geqslant \sigma_{F2}$, then

$$\Delta T_{\text{min}} = \frac{\sigma_{F2}}{d\overline{y_{F2}}/dT_1}. \tag{66}$$

Using (50) and (64),

$$\Delta T_{\text{min}} = \frac{M \left[\sum_i Q_{i,\,0} T_i^2 + 2 \sum_{i<j} V_{ij,\,0} T_i T_j \right]^{1/2}}{\sqrt{B\tau} \left\{ \sum_m C_{-m} H_{F1}(m\nu_0) P_{1,\,-m} \right\}}, \tag{67}$$

where B, τ, C_{-m}, $H_{F1}(\nu)$, $Q_{i,\,0}$, $V_{ij,\,0}$, M are defined in (53), (65), (13), (34), (19), (21), and (63) respectively.

a. Radiometers With Premultiplier Filter

Most radiometers have a narrow (compared with ν_0) bandpass filter (denoted F1 in figure 1) preceding the multiplier. For this type of radiometer the sensitivity is independent of the correlation wave form. This follows from the fact that $H_{F1}(m\nu_0)$ in (50) is zero except for $m = \pm 1$. For this case,

$$\Delta T_{\text{min}} = \frac{\left[\sum_i Q_{i,\,0} T_i^2 + 2 \sum_{i<j} V_{ij,\,0} T_i T_j \right]^{1/2}}{\sqrt{2B\tau}\, |P_{1,\,1}| \cos\psi}, \tag{68}$$

where

$$C_1 H_{F1}(\nu_0) P_{1,\,-1} \equiv |C_1 H_{F1}(\nu_0) P_{1,\,-1}| e^{i\psi}.$$

The sensitivity for particular modulation wave forms are shown in table 1.

b. Radiometers With No Premultiplier Filter

To simplify the calculations, assume the transfer function of the bandpass filter is constant in phase and amplitude and equal to $H_{F1}(\nu_0)$. In this case (67) becomes

$$\Delta T_{\text{min}} = \frac{[\overline{c^2(t)}]^{1/2} \left[\sum_i Q_{i,\,0} T_i^2 + 2 \sum_{i<j} V_{ij,\,0} T_i T_j \right]^{1/2}}{[\overline{c(t) p_1(t)}] \sqrt{B\tau}}, \tag{69}$$

where $\overline{c(t)p_1(t)}$ is introduced via (B–10) of appendix B and $\overline{c^2(t)}$ is introduced in an analogous manner.

TABLE 1. ΔT_{min} *for special ideal switching radiometers.* The amplifier noise is T_3; $Q_{3,0}=1$ for all radiometers; d is the fraction of the time the transmission coefficient differs from zero.

$$\Delta T_{\mathrm{min}}=F(B\tau)^{-1/2}\left[\sum_i Q_{i,0}T_i^2+2\sum_{i<j} V_{ij,0}T_iT_j\right]^{1/2}$$

Modulation	Correlation	F	$Q_{1,0}$	$Q_{2,0}$	$V_{12,0}$	$V_{13,0}$	$V_{23,0}$	Prior calculations
1. Square wave	sinusoidal	$\pi/\sqrt{2}$	1/2	1/2	0	1/2	1/2	a* c e*† g° j*†‡ k°
2. Square wave	square wave	2	1/2	1/2	0	1/2	1/2	e*† f° h*‡ j*†‡ k°
3. Voltage sinusoidal	sinusoidal	$2\sqrt{2}$	35/128	35/128	3/128	3/8	3/8	b*†‡ d*†‡ e*† j†‡
4. Voltage sinusoidal	square wave	π	35/128	35/128	3/128	3/8	3/8	
5. Power sinusoidal	sinusoidal	$2\sqrt{2}$	3/8	3/8	1/8	1/2	1/2	g° i* k°
6. Power sinusoidal	square wave	π	3/8	3/8	1/8	1/2	1/2	
7. Power sawtooth	sinusoidal	$\sqrt{2}\pi$	1/3	1/3	1/6	1/2	1/2	g°
8. Power sawtooth	square wave	4	1/3	1/3	1/6	1/2	1/2	
9. Rectangular	sinusoidal	$\pi/(\sqrt{2}\sin\pi d)$	d	$1-d$	0	d	1−d	
10. Rect. ($d\leqslant\frac{1}{2}$)	square wave	d^{-1}	d	$1-d$	0	d	1−d	
11. Rect. ($d\geqslant\frac{1}{2}$)	square wave	$(1-d)^{-1}$	d	$1-d$	0	d	1−d	
12. Rectangular	rectangular	$[d(1-d)]^{-1/2}$	d	$1-d$	0	d	1−d	h*‡

*Results of author conflict with this paper as noted in footnote.

°Results of author agrees in detail with this paper only when $T_1=T_2$.

†The calculation made was equivalent to assuming $T_2=0$ °K.

‡A rectangular filter bandpass assumed in calculation.

[a] Dicke [3] obtains a sensitivity greater by a factor 2 (thus ΔT_{min} less by factor 2) than this paper.

[b] Goldstein [4, 5], a minor algebraic error corrected in ref. j.

[c] Bunkin, Karlov [17].

[d] Strom [6, 7] obtains a sensitivity less by a factor $\sqrt{2}$ than this paper.

e Strum [8]. The bandpass defined does not agree with this paper except for rectangular bandpass.

[f] Kelly, Lyons, Root [11, 12] agree only when radiometer balanced.

[g] Colvin [13] agrees only for balanced, constant power radiometers.

[h] Knight [9]. Equations (3) and (4) of Knight's paper omit a factor 2π. In addition, Knight's results differ from this paper in that the terms in T_1 and T_2 do not occur.

[i] Ward and Richardson [18] obtained a sensitivity greater by a factor $2\sqrt{2}$ than this paper.

[j] Johnson [10] algebraic error for square wave modulation.

[k] Tiuri [14].

4. Special Results

A variety of particular radiometers have been considered in the literature (see sec. 2). These radiometers were listed in table 1. The radiometer types shown in table 1 are ideal in three ways. First, the switching element introduces no noise of its own, second, the maximum transmission coefficient is unity, and last, the relative phases of switching and correlation wave forms $a(t)$, $b(t)$, and $c(t)$ are selected to minimize ΔT_{min}. The factor F is equal to $2^{-1/2}|P_{1,1}|^{-1}$ for sinusoidal correlation or for radiometers with a narrow band precorrelator filter (and any reasonable correlation). These radiometers are denoted as sinusoidal correlation in table 1. For other radiometers, F is equal to $\overline{[c^2(t)]}^{1/2}\overline{[c(t)p_1(t)]}^{-1}$. Explicitly the power modulation wave forms used are

(i) square wave modulation,

$$p_1(t)=\sum_{m=-\infty}^{\infty}\frac{\sin\dfrac{m\pi}{2}}{m\pi}e^{jm2\pi\nu_0 t}; \tag{70}$$

(ii) voltage sinusoidal modulation,

$$p_1(t)=3/8+1/2\cos 2\pi\,\nu_0 t+1/8\cos 4\pi\,\nu_0 t; \tag{71}$$

(iii) power sinusoidal modulation,

$$p_1(t) = 1/2 + 1/2 \cos 2\pi \nu_0 t; \tag{72}$$

(iv) power sawtooth modulation,

$$p_1(t) = 1/2 + j \sum_{k \neq 0} (2\pi k)^{-1} e^{jk2\pi\nu_0 t}; \tag{73}$$

(v) rectangular modulation,

$$p_1(t) = \sum_k \frac{\sin k\pi d}{k\pi} e^{j2\pi p\nu_0 t}; \tag{74}$$

where d is the fraction of the time that $p_1(t)$ differs from zero. Except for voltage sinusoidal modulation, $p_2(t)$ is chosen such that $p_1(t) + p_2(t) = 1$.

4.1. Nonideal Switch

The theory developed applies to arbitrary switching wave forms. There are two common deviations from the ideal forms used for table 1. First, the nonideal power transmission coefficient, $p_i'(t)$ of the switch varies from zero to $p_{i,\,\max}$ instead of from zero to one. Thus,

$$p_i'(t) = p_{i,\,\max} p_i(t),$$

so that

$$Q_{i,\,0}' = p_{i,\,\max}^2 Q_{i,\,0}, \tag{75}$$

and

$$V_{ij,\,0}' = p_{i,\,\max} p_{j,\,\max} V_{ij,\,0}. \tag{76}$$

Equations (75) and (76) may be used in place of the corresponding ideal parameters, to extend the results of table 1 to the switch with nonideal transmission coefficient.

A second complication is that the nonideal switch radiates thermal energy in direct proportion to its temperature, and the fraction of incident energy absorbed. For a matched three-port device at temperature T_{sw}, the effective temperature of the radiation $p_{sw}(t)T_{sw}$ is [24]

$$p_{sw}(t)T_{sw} = [1 - p_1(t) - p_2(t)]T_{sw}, \tag{77}$$

where the $p_i(t)$ are given by (14). The thermal noise from the switch may be treated formally as a noise source of the temperature of the switch which is power modulated by amplitude $p_{sw}(t)$. Thus for the ideal square-wave modulation, rectangular modulation, power-sinusoidal modulation, and power-sawtooth modulation of table 1,

$$p_{sw}(t) = 0. \tag{78}$$

For ideal voltage sinusoidal modulation,

$$p_{sw}(t) = \frac{1}{4} - \frac{1}{4} \cos 4\pi\nu_0 t. \tag{79}$$

TABLE 2. *Balanced, constant switched power, nonideal radiometer sensitivities.*

The maximum power transmission coefficient through the switch is $p_{1,\,\max}=p_{2,\,\max}=\alpha$; $T_1=T_2$; the effective amplifier noise is T_n; and the physical temperature of the switch is T_{sw}.

$$\Delta T_{\min}=F\,\frac{T_1+\alpha^{-1}T_n+(\alpha^{-1}-1)T_{sw}}{\sqrt{B\tau}}$$

A. Narrow band precorrelator filter or sinusoidal correlation

Modulation	F
Square wave	$\pi/\sqrt{2}=2.22$
Power sinusoidal	$2\sqrt{2}=2.83$
Power sawtooth	$\sqrt{2}\pi=4.44$
Rectangular*	$\pi/(\sqrt{2}\sin\pi d)$

B. No precorrelator filter

Modulation	Correlation	F
Square wave	square wave	2
Power sinusoidal	square wave	π
Power sawtooth	square wave	4
Rectangular*	rectangular	$[d(1-d)]^{-1/2}$
Rectangular* ($d\leq\frac{1}{2}$)	square	d^{-1}
Rectangular* ($d\geq\frac{1}{2}$)	square	$(1-d)^{-1}$

*d is the fraction of the time the transmission coefficient is different than zero.

4.2. Balanced Radiometers With Nonideal Switches

The expression for $\Delta T_{\min}$ simplifies when the noise sources being compared have nearly the same effective temperature and when the power to the amplifier is constant [i.e., $p_1(t)+p_2(t)$ $=$constant]. Table 2 lists the results for radiometers having nonideal switches that satisfy these special conditions. The sensitivity indicated is for the correlation phase which minimizes $\Delta T_{\min}$.

The $\Delta T_{\min}$ for the voltage sinusoidally modulated radiometer does not simplify for $T_1=T_2$. However, for a radiometer with a narrow band precorrelator filter (or sinusoidal correlation) and a switch where the maximum power transmission coefficients $p_{1,\,\max}=p_{2,\,\max}=\alpha$, $\Delta T_{\min}$ for $T_1=T_2$ is bounded by the following expressions:

$$\Delta T_{\min}>2\sqrt{2}\,\frac{\left[\frac{3}{4}T_1+\alpha^{-1}T_3+\left(\alpha^{-1}-\frac{7}{8}\right)T_{sw}\right]}{\sqrt{B\tau}},\tag{80}$$

and

$$\Delta T_{\min}<2\sqrt{2}\,\frac{\left[\frac{7}{8}T_1+\alpha^{-1}T_3+\left(\alpha^{-1}-\frac{3}{4}\right)T_{sw}\right]}{\sqrt{B\tau}}.\tag{81}$$

For no precorrelator filter and square wave correlation, $2\sqrt{2}$ is replaced by π.

5. Experimental Procedure

The sensitivity of a Dicke radiometer similar to Wells, Daywitt, and Miller [1] was determined experimentally. A switchable circulator was used for the switch instead of a magic tee and motor driven attenuators. The switchable circulator provided square-wave modulation at 1000 Hz. The 30 MHz output of the IF amplifier was attenuated by various amounts and then fed to a crystal detector. The detector law of this detector is shown in figure 2. The arrows indicate operating points for which the radiometer sensitivity was measured. The numbers near the arrows are the minimum resolvable temperature changes measured for each level.

The mixer-preamplifier-IF amplifier voltage response is shown for one channel in figure 3. The other channel is similar. The markers along the bottom of the figure are synthesized at 2 MHz intervals. The convolution bandwidth was calculated using a computer program based on (53). The system bandwidth is determined from a single channel response as discussed in appendix C.

The time constant for the low pass filter of the lock-in amplifier nominally set at 10 sec integrating time is based on the voltage response measurement shown in figure 4.

The recorded data were plotted on probability paper. The ordinate of this paper is the amplitude (voltage) of the radiometer output, and the abscissa is the percent of the time the recorder trace exceeds the ordinate value. The scale of the paper makes the plot a straight line if the data have normal (Gaussian) distribution. From the plot, the mean of the data is the value of the ordinate for which the abscissa is 50 percent. The standard deviation σ (for normal distribution) is the difference in the ordinate values for abscissa values of 50 percent and 84.1 percent (or 15.9% and 50%). Figure 5 shows two sets of data, one before and one after a change of 0.0087 dB (21.6 °K change from 10,800 °K) of input power is made in one noise source.

The various parameters for the radiometer under test are given in table 3. The theoretical ΔT_{min} is based on table 2 for the balanced radiometer using square-wave modulation. The experimental ΔT_{min} is the mean result of $\Delta T_1/(\overline{\Delta y_{F2}}/\sigma_{F2})$ taken from four plots similar to figure 5 for a $\Delta T_1 = 21.6$ °K.

A feature common to all data and shown in figure 5 is an increase in σ when the noise power decreases from null. No change in σ is noticeable when the noise power increases (out to 0.2 dB change). The cause of this feature is not known.

The radiometer sensitivity as noted in figure 2 for the radiometer at various operating points are comparable.

6. Conclusions

The areas of agreement within the literature have been ferreted out and the nature of discrepancies determined. A new analysis of the Dicke radiometer was presented which was general enough to include all of the papers reviewed as a special case and to extend the sensitivity calculations to include radiometers with a lossy switch.

The most sensitive radiometer is a square-wave modulated radiometer with wide band (i.e., no premultiplier filter) square-wave correlator. However, the potential 11 percent advantage in sensitivity for wide band square-wave correlation over systems using a narrow premultiplier filter must be weighed against the practical difficulties associated with wide band systems. Also the narrow band correlator insures that the output of the radiometer is proportional to the difference of input powers [i.e., to $T_1 - T_2$; see eq (50)] independent of the asymmetry of the modulation.

The sensitivity of a square-wave modulated radiometer using a narrow precorrelator filter was determined experimentally. The measured sensitivity was the same as the theoretical radiometer using a full-wave, square-law detector. The sensitivity of the radiometer was independent (within the experimental error) of whether a half-wave square-law, linear, or intermediate-law detector was used.

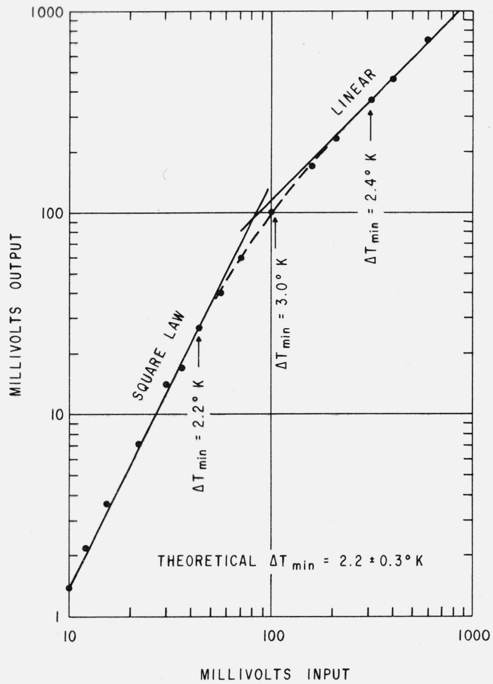

FIGURE 2. *Detector law.*

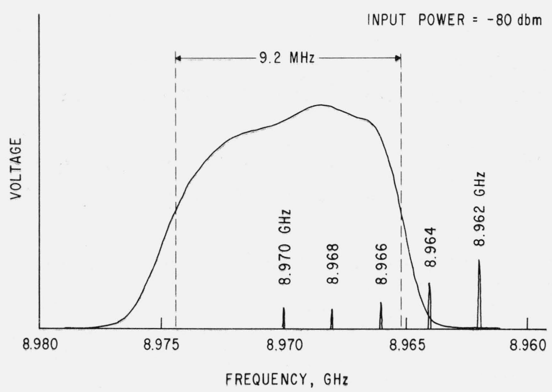

FIGURE 3. *Amplifier voltage response.*

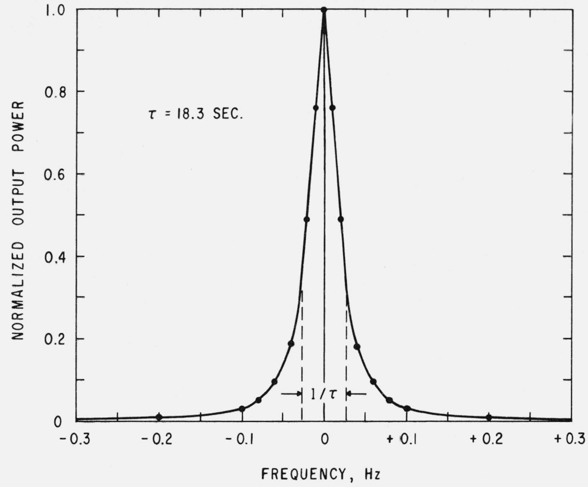

FIGURE 4. *Power response of the low pass filter.*

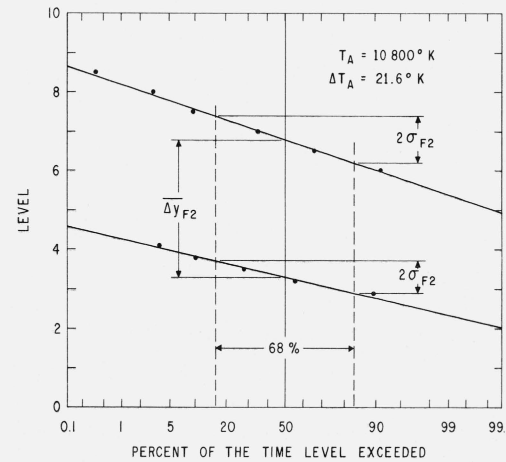

FIGURE 5. *Data plotted on probability paper.*

TABLE 3. *Parameters of the Dicke radiometer under test*

Predetection bandwidth (B)	9.2 MHz ± 10%
Postdetection integrating time (τ)	18 sec ± 10%
Receiver noise temperature (T_n)	750 °K ± 5%
Maximum switch transmission (α)	$(2.57)^{-1}$ ± 4%
Switch temperature (T_{SW})	295 °K
Noise sources ($T_1 \simeq T_2$)	10,800 ± 2.5%
Switching frequency (ν_0)	1000 Hz
Switching waveform	Square wave
Microwave frequency (local oscillator)	9 GHz
ΔT_{min} (theory)	2.3 °K ± 15%
ΔT_{min} (experimental)	2.3 °K ± 20%

The author thanks Charles L. Trembath and Douglas W. Schulze for carrying out the experimental measurements and Bernice K. Bender for the bandwidth computer program. Discussions with John J. Faris and Glenn F. Engen were very useful. Comments by M. E. Tiuri and the use of a preprint and comments by Walter A. Johnson were helpful. This research was supported by the Advanced Research Projects Agency under Project DEFENDER and was monitored by Charles M. Herzfeld under ARPA Order No. 515.

7. Appendix A. Equivalent Statements for B and τ and Notation Conversion for Literature

Various statements are used in the literature for B and τ. This section gives the definition used in this paper in alternate forms which are easier to compare with the literature.

Using the Wiener-Khintchine Theorem, (7), and assuming the order of integration can be interchanged, the following relationships can be proven:

$$G(0)\bigstar G(0)=\int_{-\infty}^{\infty} G^2(\nu)d\nu, \tag{A-1}$$

$$\int_{-\infty}^{\infty} G(\nu)\bigstar G(\nu)d\nu=\left[\int_{-\infty}^{\infty} G(\nu)d\nu\right]^2, \tag{A-2}$$

$$g(0)=\int_{-\infty}^{\infty} G(\nu)d\nu, \tag{A-3}$$

$$H(0)=\int_{-\infty}^{\infty} h(t)dt, \tag{A-4}$$

and Parsevals relation,

$$\int_{-\infty}^{\infty} H(\nu)H^*(\nu)d\nu=\int_{-\infty}^{\infty} h^2(t)dt, \tag{A-5}$$

where $g(t)$ is the Fourier transform (autocorrelation function) of the power response $G(\nu)$, and $h(t)$ and $H(\nu)$ are a Fourier transform pair, with $h(t)$ a real function.

If instead of using frequency ν in hertz (cycles per second) as a parameter, the angular frequency $\omega=2\pi\nu$ is used, then the following conversions may be used:

$$\nu=\omega/(2\pi),$$

$$G_\nu(\nu)=2\pi G_\omega(\omega),$$

$$W_\nu(\nu)=2\pi W_\omega(\omega),$$

$$Y_\nu(\nu)=2\pi Y_\omega(\omega),$$

$$H_\nu(\nu)=2\pi H_\omega(\omega),$$

$$G_\nu(\nu)\bigstar G_\nu(\nu)=2\pi G_\omega(\omega)\bigstar G_\omega(\omega),$$

where the subscripts ν and ω are introduced to distinguish a difference in functional form. This subscript will now be dropped. The functional form appropriate to the function used is understood. The conversion from $W(\nu)$ to $W(\omega)$ is chosen so that

$$W(\nu)d\nu = W(\omega)d\omega.$$

In the ω notation,

$$Y(\omega) = (2\pi)^{-1} \int_{-\infty}^{\infty} e^{-j\omega t} y(t)dt,$$

and

$$W(\omega) = \lim_{T\to\infty} (2\pi/T)Y(\omega)Y^*(\omega).$$

The conversion system above is not unique. The easiest way to determine what system a given author is using is by examining the form used for the Wiener-Khintchine theorem, or statements which include the autocorrelation function. The autocorrelation function is universally defined in a manner equivalent to (9).

7.1. Equivalent Statements for B

The definition of B is in (52):

$$B = \frac{\left[\int_{-\infty}^{\infty} G_A(\nu)d\nu\right]^2}{2G_A(0)\bigstar G_A(0)}. \tag{A-6}$$

Using (A–2),

$$B = \frac{\int_{-\infty}^{\infty} G_A(\nu)\bigstar G_A(\nu)d\nu}{2G_A(0)\bigstar G_A(0)}, \tag{A-7}$$

or (A–1),

$$B = \frac{\left[\int_{-\infty}^{\infty} G_A(\nu)d\nu\right]^2}{2\int_{-\infty}^{\infty} G_A^2(\nu)d\nu}. \tag{A-8}$$

Beginning with (A–8), noting that $G_A(\nu) \equiv H_A(\nu)H_A^*(\nu)$, and converting to ω notation,

$$B = \frac{\left[\int_{-\infty}^{\infty} |H_A(\omega)|^2 d\omega\right]^2}{4\pi \int_{-\infty}^{\infty} |H_A(\omega)|^4 d\omega}. \tag{A-9}$$

Beginning with (A–8), applying (A–3) to the numerator and (A–5) to the denominator,

$$B = \frac{g_A^2(0)}{2\int_{-\infty}^{\infty} g_A^2(t)dt}. \tag{A-10}$$

Using a normalized autocorrelation function, $\rho_A(t)=g_A(t)/g_A(0)$,

$$(2B)^{-1}=\int_{-\infty}^{\infty}\rho_A^2(t)dt. \tag{A-11}$$

7.2. Equivalent Statements for τ

The definition of τ is from (65):

$$\tau^{-1}=\int_{-\infty}^{\infty}G_{F2}(\nu)d\nu/G_{F2}(0). \tag{A-12}$$

Noting that $G_{F2}(\nu)\equiv H_{F2}(\nu)H_{F2}^*(\nu)$ and converting to the ω convention,

$$\tau^{-1}=\frac{\int_{-\infty}^{\infty}|H_{F2}(\omega)|^2d\omega}{2\pi H_{F2}^2(\omega=0)}. \tag{A-13}$$

Using (A–4), and (A–5), and assuming a causal system such that $h(t)=0$ for $t<0$,

$$\tau^{-1}=\frac{\int_{-\infty}^{\infty}h_{F2}^2(t)dt}{\left[\int_{-\infty}^{\infty}h_{F2}(t)dt\right]^2}. \tag{A-14}$$

7.3. Literature Conversion

Several representative statements from the literature referring to the minimum resolvable change in temperature for a radiometer near balance ($T_1=T_2$) and for $\Delta T_{\min}\leqslant T_n$ will be converted to the notation of this paper.

a. Dicke [1946]

Dicke's [3] equation (21) for square-wave modulation and cosine correlation is,

$$\frac{\Delta T}{T}=\frac{\pi}{2}N\frac{\left\{\left[\int_{-\infty}^{\infty}|F(\omega)|^4d\omega\right]\left[\int_{-\infty}^{\infty}|S(\omega)|^2d\omega\right]\right\}^{1/2}}{S(0)\int_{-\infty}^{\infty}|F(\omega)|^2d\omega}. \tag{A-15}$$

Using (A–9) and (A–13) and the following conversions,

$$\Delta T=\Delta T_{\min},$$

$$T=T_1=T_2,$$

$$N=(T_n+T_1)/T_1 \text{ (for } T_1=290\ ^\circ\text{K)},$$

$$F(\omega)=H_A(\omega),$$

$$S(\omega)=H_{F2}(\omega),$$

and (A–15) becomes

$$\Delta T_{\min}=\pi(T_1+T_n)(8B\tau)^{-1/2}.$$

b. Goldstein [1955, 1956]

For voltage sinusoidal modulation and sinusoidal correlation Goldstein [4, 5] obtains

$$\sigma_{Id}^2 = 4\sigma_n^2 \sqrt{\gamma/\alpha}. \tag{A–16}$$

Goldstein's work corresponds to $T_1 = T_2 = 0$ °K and

$$\sigma_{Id}^2 = k\Delta T_{\text{min}},$$

$$\sigma_n^2 = kT_n,$$

$$\gamma = (2\tau)^{-1},$$

$$\alpha = B,$$

where k is Boltzman's constant. Thus (A–16) becomes

$$\Delta T_{\text{min}} = 4T_n(2B\tau)^{-1/2}.$$

c. Bunkin and Karlov [1955]

For square-wave modulation and sinusoidal correlation, Bunkin and Karlov obtain [17]

$$\delta T = \pi(T_{\text{in}} + T_e)\left\{\frac{1}{\Delta\omega}\frac{\Delta\Omega_1\Delta\Omega}{\Delta\Omega_1 + \Delta\Omega}\left[1 + \frac{\Delta T}{T_{\text{in}} + T_e} + \frac{1}{2}\frac{\Delta T^2}{(T_{\text{in}} + T_e)^2}\right]\right\}^{1/2}. \tag{A–17}$$

If the precorrelator bandwidth $\Delta\Omega_1$ is much greater than the postcorrelator low pass filter bandwidth $\Delta\Omega$, then

$$\frac{\Delta\Omega_1\Delta\Omega}{\Delta\Omega_1 + \Delta\Omega} \approx \Delta\Omega.$$

Using the following conversions

$$\delta T = \Delta T_{\text{min}},$$

$$T_{\text{in}} = T_n,$$

$$T_e = T_1,$$

$$\Delta\omega = 2\pi B,$$

$$\Delta\Omega = \pi/\tau,$$

for $\Delta T \ll 1$, (A–17) becomes

$$\Delta T_{\text{min}} = \pi(T_1 + T_n)(2B\tau)^{-1/2}.$$

d. Kelly, Lyons, and Root [1958, 1963]

For square-wave modulation and detection, (49) and (31) of Kelly, Lyons, and Root [12] becomes

$$\Delta T = 2[T_2 + T_n]\sqrt{\frac{1 + \Gamma(0)}{B\tau}}. \tag{A–18}$$

Equations (A–11) and (A–14) are used to establish the conversion for B and τ. Using the following conversions,

$$\Delta T=\Delta T_{\text{min}},$$

$$T_2=T_2=T_1,$$

$$T_n=T_n,$$

$$\Gamma(0)=0, \text{ (for zero gain fluctuations)}$$

$$B=B,$$

$$\tau=\tau,$$

(A–18) becomes

$$\Delta T_{\text{min}}=2(T_1+T_n)(B\tau)^{-1/2}.$$

e. Knight [1962]

For rectangular modulation and rectangular correlation, Knight [9] obtains

$$\frac{S}{N}=\frac{2\pi\,\alpha(\sigma_R^2-\sigma_S^2)^2}{2\Gamma\sigma_N^4}\left(\frac{a}{a+b}\right)\left(1-\frac{a}{a+b}\right), \tag{A–19}$$

where the 2π omitted in Knight's eq (4) is added. The appropriate resolution criterion is $S/N=1$. With this condition, then

$$\sigma_R^2-\sigma_S^2=k\Delta T_{\text{min}},$$

$$\sigma_N^2=kT_n,$$

$$a/(a+b)=d,$$

$$\Gamma=\pi/\tau,$$

$$\alpha=B,$$

and (A–19) becomes

$$\Delta T_{\text{min}}=T_n[B\tau d(1-d)]^{-1/2}$$

8. Appendix B. Theorems on the Fourier Transtorm

Several theorems involving the Fourier transform of the time function $y_x(t)$ and $y_z(t)$ of zero mean are proved in this appendix:

$$\operatorname*{Lim}_{T\to\infty}\frac{Y_x(\nu)Y_z^*(\nu)}{T}=0, \tag{B–1}$$

for $y_x(t)$ uncorrelated with $y_z(t)$, and

$$\lim_{T\to\infty} \frac{1}{T} Y_{xz}(\nu) Y^*_{x'z'}(\nu') = 0, \tag{B-2}$$

unless $y_x(t) \equiv y'_x(t)$, $y_z(t) \equiv y'_z(t)$, and $\nu = \nu'$, and

$$\bar{y} = \lim_{T\to\infty} \frac{Y(0)}{T}, \tag{B-3}$$

and

$$\lim_{T\to\infty} \frac{Y_{xx}(0)}{T} = \int_{-\infty}^{\infty} W_x(\nu) d\nu, \tag{B-4}$$

and

$$Y_x(\nu + p\nu_0) \bigstar Y_z(\nu + q\nu_0) = Y_{xz}(\nu + p\nu_0 + q\nu_0), \tag{B-5}$$

and

$$P_{i,r} = \frac{1}{\Theta} \int_{-\Theta/2}^{\Theta/2} a_i^2(t) e^{j2\pi r \nu_0 t} dt, \tag{B-6}$$

and

$$P_{i,r} = \sum_{m=-\infty}^{\infty} A_{i,m} A_{i,r-m}, \tag{B-7}$$

and

$$Q_{i,0} = \sum_m P_{i,m} P^*_{i,m}, \tag{B-8}$$

and

$$V_{ij,0} = \sum_m U_{ij,m} U^*_{ij,m}, \tag{B-9}$$

where $P_{i,r}$ and $A_{i,p}$ are defined in (18) and (12) respectively, and $\Theta = \nu_0^{-1}$ is one period of the periodic signal $p(t)$, and

$$\sum_\alpha C_\alpha P_{1,-\alpha} = \overline{c(t) p_1(t)} \tag{B-10}$$

where

$$\overline{c(t) p_1(t)} \equiv \frac{1}{\Theta} \int_{-\Theta/2}^{\Theta/2} c(t) p_1(t) dt. \tag{B-11}$$

8.1. Theorem 1

Taking the inverse transform (3) of the left-hand side of (B–1), then taking inverse transform of $Y_1(\nu)$ *and* $Y_2(\nu)$ *and interchanging the order of integration, one obtains* (Lim $T \to \infty$ *is understood*)

$$T^{-1} \int_{-\infty}^{\infty} e^{j2\pi\nu t} Y_1(\nu) Y_2^*(\nu) d\nu = T^{-1} \iint y_1(t') y_2(t') dt' dt'' \int_{-\infty}^{\infty} e^{j2\pi\nu(t - t' + t'')} d\nu.$$

The integration over ν yields the Dirac delta function $\delta(t-t'+t'')$ *[24].*

Thus integrating over t',

$$T^{-1}\int e^{j2\pi\nu t}Y_1(\nu)Y_2^*(\nu)d\nu = T^{-1}\int_{-\infty}^{\infty} y_1(t+t'')y_2(t'')dt''.$$

If $y_1(t)$ *and* $y_2(t)$ *are not correlated, then the integral on the right is finite, and when divided by* T *tends to zero as* $T\to\infty$. *Thus, the left-hand side is zero, the Fourier transform is also zero and (B–1) is proved.*

8.2. Theorem 2

The theorem is proved in a manner analogous to theorem 1.

8.3. Theorem 3

By definition,

$$\bar{y} = \lim_{T\to\infty}\frac{1}{T}\int_{-T/2}^{T/2} y(t)dt.$$

The function $y(t)$ *is truncated so that* $y(t)$ *equals zero for* $|t| > T/2$. *Thus,*

$$\bar{y} = \lim_{T\to\infty}\frac{1}{T}\int_{-\infty}^{\infty} y(t)dt.$$

Taking the Fourier transform of $y(t)$ *and interchanging the order of integration,*

$$\bar{y} = \lim_{T\to\infty}\frac{1}{T}\int_{-\infty}^{\infty} Y(\nu)d\nu\int_{-\infty}^{\infty} e^{j2\pi\nu t}dt.$$

The integration over time yields the δ-function of ν. Subsequent integration over ν yields (B–3).

8.4. Theorem 4

Let $Y_{xz}(\nu)$ *be the Fourier transform of* $y_x(t)y_z(t)$ *where* $y_x(t)$ *and* $y_z(t)$ *are random variables with zero mean:*

$$Y_{xz}(\nu) = \int_{-\infty}^{\infty} e^{-j2\pi\nu t}y_x(t)y_z(t)dt.$$

If $y_x(t)$ *is not correlated to* $y_z(t)$ *or* $e^{-j2\pi\nu t}$, *then the mean of the product is zero. Thus,* $Y_{xz}(\nu)$ *is finite and if divided by* T, *will approach zero as* $T\to\infty$. *If* $y_z(t)\equiv y_x(t)$, *then*

$$Y_{xx}(\nu) = \int_{-T/2}^{T/2} e^{-j2\pi\nu t}y_x^2(t)dt,$$

where the limits of the integral are taken from $-T/2$ *to* $T/2$. *This does not change the value of the integral because* $y(t)=0$ *for* $|t|\geqslant T/2$. *When* $y_x^2(t)$ *is rewritten as* $\overline{y_x^2}+[y_x^2(t)-\overline{y_x^2}]$ *and the above equation is divided by* T *(the limit* $T\to\infty$ *being understood),*

$$T^{-1}Y_{xx}(\nu) = T^{-1}\left\{\overline{y_x^2}\int_{-T/2}^{T/2} e^{-j2\pi\nu t}dt + \int_{-T/2}^{T/2} e^{-j2\pi\nu t}[y_x^2(t)-\overline{y_x^2}]dt\right\}.$$

247-602 O-67—5

The integral in the second term is finite and the term goes to zero as $T \rightarrow \infty$. *The first term on the right-hand side goes to zero unless* $\nu = 0$. *For* $\nu = 0$ *the term approaches* $\overline{y_x^2}$. *Thus,*

$$\lim_{T \to \infty} Y_{xz}(\nu) = \begin{cases} \overline{y_x^2} & \textit{for } \nu = 0 \textit{ and } x = z, \\ 0 & \textit{otherwise.} \end{cases}$$

Using (10) yields (B–4).

8.5. Theorem 5

Using the definition of convolution, eq (5),

$$Y_x(\nu + m\nu_0) \bigstar Y_z(\nu + q\nu_0) \equiv \int_{-\infty}^{\infty} Y_x(\nu' + m\nu_0) Y_z(\nu - \nu' + q\nu_0) d\nu'.$$

Taking the Fourier transform and interchanging the order of integrations,

$$Y_x(\nu + m\nu_0) \bigstar Y_z(\nu + q\nu_0) = \int\int_{-\infty}^{\infty} e^{-j2\pi[m\nu_0 t + \nu t' + q\nu_0 t']} y_x(t) y_z(t') dt\, dt' \cdot \int_{-\infty}^{\infty} e^{-j2\pi\nu''(t-t')} d\nu'.$$

The integration over ν' *yields* $\delta(t - t')$, *then the result of integrating over* t' *is identified as* $Y_{xz}(\nu + m\nu_0 + q\nu_0)$.

8.6. Theorem 6

To obtain (B–6), both sides of (18) are multiplied by $e^{j2\pi r\nu_0 t}$ *and then integrated over a period, using for* $p_i(t)$ *the equivalent* $a_i^2(t)$ *as noted in (14).*

8.7. Theorem 7

Using (B–6) and (12),

$$P_{i,r} = \frac{1}{\Theta} \sum_{m,s} \int_{-\Theta/2}^{\Theta/2} [A_{i,m} e^{jm2\pi\nu_0 t}][A_{i,s} e^{j(s-r)2\pi\nu_0 t}] dt.$$

Due to the orthogonality of different Fourier components, the integral has nonzero value only when $s = r - m$. *This leads directly to (B–7).*

8.8. Theorems 8, 9, 10, and 11

The proof of (B–8), (B–9), and (B–10) are analogous to the proof of (B–7). Equations (13), through (21) are needed for various definitions.

9. Appendix C. Radiometer Using an IF Amplifier

A schematic for the IF amplifier is shown in figure C–1. Instead of the amplifier shown in figure 1, now a mixer, local oscillator, and IF amplifier are used. The amplifier noise temperature T_n of figure 1 is now interpreted as the noise temperature of the mixer-IF amplifier as referred to the input of the *mixer*. Using the same notation convention as the body of the paper,

$$\begin{aligned} y_{LO}(t) &= \eta \cos 2\pi\nu_1 t, \\ y_{SM}(t) &= \eta y_S(t) \cos 2\pi\nu_1 t, \qquad \text{(C–1)} \\ y_A(t) &= h_A(t) \bigstar y_{SM}(t), \end{aligned}$$

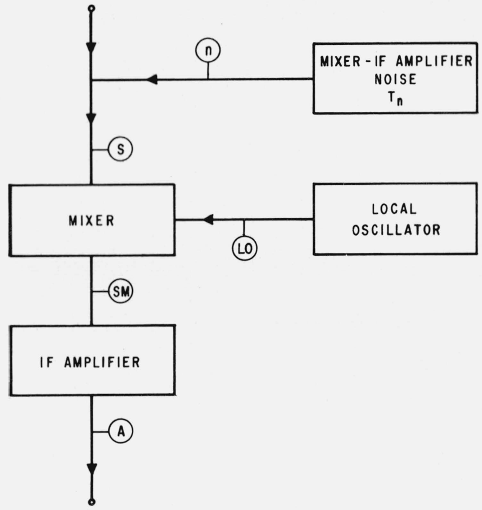

FIGURE C–1. *IF amplifier.*

where η is the amplitude of the local oscillator of frequency ν_1. From (C–1), it is clear that an ideal balanced mixer is assumed. Taking the Fourier transform,

$$Y_{SM}(\nu)=\tfrac{1}{2}\eta\,[Y_S(\nu+\nu_1)+Y_S(\nu-\nu_1)], \tag{C–2}$$

$$Y_A(\nu)=H_A(\nu)Y_{SM}(\nu). \tag{C–3}$$

Applying (6),

$$W_{SM}(\nu)=(\eta^2/4)[W_S(\nu+\nu_1)+W_S(\nu-\nu_1)], \tag{C–4}$$

$$W_A(\nu)=G_A(\nu)W_{SM}(\nu). \tag{C–5}$$

9.1. Calculation of $\overline{y_{F2}}$

The calculation of $\overline{y_{F2}}$ proceeds in a manner similar to section 3.5 except (C–2) and (C–3) are used in place of (29). Thus, instead of (46), now we have,

$$Y_A(\nu)=\tfrac{1}{2}\eta\sum_{i,p}A_{i,\,-p}[Y_{i\bigstar A}(\nu+p\nu_0+\nu_1)+Y_{i\bigstar A}(\nu+p\nu_0-\nu_1)]. \tag{C–6}$$

Substituting (C–6) into (30) will give terms of the type [see eq (47)],

$$Y_x(\nu+m\nu_0\pm\nu_1)\bigstar Y_z(\nu+q\nu_0\mp\nu_1)=Y_{xz}(\nu+m\nu_0+q\nu_0)$$

and

$$Y_x(\nu+m\nu_0\pm\nu_1)\bigstar Y_z(\nu+q\nu_0\pm\nu_1)=Y_{xz}(\nu+m\nu_0+q\nu_0\pm 2\nu_1). \tag{C–7}$$

Using an argument similar to that used to obtain (48), noting that the terms like (C–7) do not contribute,

$$\lim_{T\to\infty}\frac{Y_D(m\nu_0)}{T}=\frac{1}{2}\eta^2\sum_{i,\,q}A_{i,\,q}A_{i,\,-q-m}K_{i\bigstar A}. \tag{C–8}$$

Equation (C–8) is identical to (48) except for the multiplicative constant $\frac{1}{2}\eta^2$. Thus the remainder of the calculation is unchanged except that the gain functions λ of (51) now contain $\frac{1}{2}\eta^2$. Thus,

$$\lambda=\tfrac{1}{4}\eta^2kH_{F2}(0)[2G_A(0)\bigstar G_A(0)]^{1/2}. \tag{C–9}$$

9.2. Calculation of σ_{F2}

The calculation of σ_{F2} proceeds in a manner similar to section 3.5 except (C–4) and (C–5) are used in place of (37). Because $W_S(\nu+\nu_1)=W_S(\nu-\nu_1)$, (C–4) and (C–5) combined become,

$$W_A(\nu)=\tfrac{1}{2}\eta^2 G_A(\nu)W_S(\nu).$$

Thus the calculation is similar except $W_S(\nu)$ is replaced by $\frac{1}{2}\eta^2 W_S(\nu)$. If (C–9) is used for the definition of λ, then the statement of $\overline{y_{F2}}$ and σ_{F2} in (50) and (64) are otherwise unchanged.

9.3. Comments

The bandwidth B is defined in a similar manner whether the amplifier is at the signal frequency or an IF frequency. For an IF amplifying system, B is the bandwidth of the IF amplifier. If for some reason the signal were only in the signal channel of the IF amplifier (the noise remains in both channels), then T_1 and T_2 would be replaced by $\frac{1}{2}T_1$ and $\frac{1}{2}T_2$, but no other changes. Thus, the single channel IF radiometer would be equivalent (as far as sensitivity is concerned) to a similar double-channel IF radiometer except it would have twice the amplifier noise temperature.

10. References

[1] J. S. Wells, W. C. Daywitt, and C. K. S. Miller, Measurement of effective temperatures of microwave noise sources, IEEE Trans. on Instr. and Meas. **IM–13,** 17–28 (Mar. 1964).

[2] D. F. Wait, and C. L. Trembath, A comparison between a switched and a correlation radiometer for cryogenic noise source measurements, ISA Conference, Los Angeles, California, Preprint No. 14.4–3–65 (Oct. 1965).

[3] R. H. Dicke, The measurement of thermal radiation at microwave frequencies, Rev. Sci. Inst. **17,** 268–275 (July 1946).

[4] S. J. Goldstein, Jr., A comparison of two radiometer circuits, Proc. IRE **43,** 1663–1666 (Nov. 1955).

[5] S. J. Goldstein, Jr., A comparison of two radiometer circuits, Proc. IRE **44,** 366 (Mar. 1956).

[6] L. D. Strom, The theoretical sensitivity of the microwave radiometer, a problem in non-stationary noise analysis, Doctoral Thesis, University of Texas (1957).

[7] L. D. Strom, The theoretical sensitivity of the Dicke radiometer, Proc. IRE **45,** No. 9, 1291–1292 (1957).

[8] P. D. Strum, Considerations in high-sensitivity microwave radiometry, Proc. IRE **46,** 43–53 (Jan. 1958).

[9] J. Knight, A general expression for the output of a Dicke-type radiometer, Proc. IRE **50,** No. 12, 2497–2498 (1962).

[10] W. A. Johnson, Effect of modulation-correlation choices on Dicke radiometer performance, Proc. IEEE **52,** 1242–1243 (1964).

[11] E. J. Kelly, D. H. Lyons, and W. L. Root, The theory of the radiometer, MIT Lincoln Lab. Group 312 Group Report 47.16 (May 1958).

[12] E. J. Kelly, D. H. Lyons, and W. L. Root, The sensitivity of radiometric measurements, J. Soc. Indust. Appl. Math. **11,** 235–257 (1963).

[13] R. S. Colvin, A study of radio astronomy receivers, Stanford Radio Astronomy Institute Publication **18A,** Stanford Electronics Labs., Stanford University [AF 18(603)–53] (Oct. 1961).

[14] M. E. Tiuri, Radio astronomy receivers, IEEE Trans. on Mil. Electro. **MIL–8,** 264–272 (1964).

[15] S. O. Rice, Mathematical analysis of random noise, Bell Sys. Tech. J. **23,** 282–332 (1944); Bell Sys. Tech. J. **24,** 46–156 (1945).

[16] W. Selove, A dc comparison radiometer, Rev. Sci. Instr. **25,** No. 2, 120–123 (Feb. 1954).

[17] F. V. Bunkin, and N. V. Karlov, On the question of sensitivity of radiometers (in Russian), Zhur, Tekh. Fiz. **25,** 430–435, 733–741 (1955).

[18] G. D. Ward, and J. M. Richardson, Analysis of a microwave radiometer for precise standardization of noise sources, J. Res. NBS **67C** (Engr. and Instr.), No. 2, 139–159 (1963).

[19] J. L. Lawson, and G. E. Uhlenbeck, Threshold signals **24,** MIT Rad. Lab. Series (McGraw-Hill Book Co., New York, N.Y., 1950).

[20] Y. W. Lee, Statistical theory of communication (John Wiley & Sons, Inc., New York, N.Y., 1960).

[21] H. Nyquist, Thermal agitation of electric charge in conductors, Phys. Rev. **32,** 110–113 (1928).

[22] B. M. Oliver, Thermal and quantum noise, Proc. IEEE **53,** 436–454 (1965).

[23] M. J. Lighthill, Fourier analysis and generalized functions, Cambridge (1960), or A. Messiah, Quantum mechanics (North Holland Publishing Co., Amsterdam, Holland), p. 468 (1961).

[24] D. F. Wait, Noise from passive multiports, to be published.

(Paper 71C2–252)